A Computer Vision-Based Approach for Non-contact Modal Analysis and Finite Element Model Updating

A COMPUTER VISION-BASED APPROACH FOR NON-CONTACT MODAL ANALYSIS AND FINITE ELEMENT MODEL UPDATING

Marco Civera[1], Luca Zanotti Fragonara[2] and Cecilia Surace[3]

[1] Department of Mechanical and Aerospace Engineering-DIMEAS, Politecnico di Torino, Corso Duca degli Abruzzi 24, 10129 Turin, Italy; marco.civera@polito.it
[2] Centre for Autonomous and Cyber-Physical Systems, Cranfield University, Cranfield, Bedford MK43 0AL, UK; l.zanottifragonara@cranfield.ac.uk
[3] Department of Structural, Geotechnical and Building Engineering-DISEG, Politecnico di Torino, Corso Duca degli Abruzzi 24, 10129 Turin, Italy; cecilia.surace@polito.it

Abstract. Computer vision-based techniques for modal analysis and system identification are rapidly becoming of great interest for both academic research and engineering practice in structural engineering. For instance, this is particularly relevant in fields such as bridge or tall building monitoring, where the large size of the structure would require an expensive sensor network, and for the characterisation of very slender, highly-flexible structural components, where physically-attached sensors cannot be deployed without altering the mass and stiffness of the system under investigation. This study concerns the latter case. Here, an algorithm for the full-field, non-contact extraction and processing of useful information from vibrational data is applied. Firstly, video acquisition is used to capture rapidly very spatially- and temporally-dense information regarding the vibrational behaviour of a high-aspect-ratio (HAR) prototype wing, with high image quality and high frame rate. Video processing is then applied to extract displacement time histories from the collected data; in turn, these are used to perform Modal Analysis (MA) and Finite Element Model Updating (FEMU). Results are benchmarked against the ones obtained from a single-point laser Doppler vibrometer (LDV). The study is performed on the beam-like spar of the wing prototype with and without the sensors attached to appreciate the disruptive effects of sensor loading. Promising results were achieved.

Keywords: parameter estimation; model updating; system identification; video processing; computer vision; experimental modal analysis.

1 Introduction

To perform realistic numerical simulations, a reliable predictive Finite Element Model (FEM) is required. To achieve such a FEM, the unknown material parameters of the corresponding real-life system need to be estimated from experimental acquisitions. This is generally achieved by attaching mounted sensors, such as accelerometers, to the structure of interest. However, this classic experimental setup has at least two main disadvantages. Firstly, it only allows a sparse, point-wise disposition of the

output channels, which limits the amount of available information. Secondly, both the additional weight of and the additional stiffness induced by the physically attached transducers and by their connection to the investigated system affect the dynamical response of the structure-sensors ensemble. The first issue negatively affects the robustness and reliability of the model since it is derived from relatively few recordings. Indeed, while the global dynamic behaviour can be estimated even from few points, the lack of local information severely hampers some more specific investigations, such as damage localisation, where high or very high spatial density is required [1], [2]. Regarding the latter point, the effects of the additional masses and stiffness are negligible on massive buildings such as bridges or bell towers, yet become predominant for very lightweight, very slender structural elements. This is especially relevant for the aeronautical industry, where in recent years more and more efforts have been dedicated to producing lighter and more flexible wings [3]. Thus, the recorded behaviour of the system-sensors ensemble can diverge substantially (both locally and globally) from the one corresponding to the system alone with no transducers attached.

The linear dynamics of the XB-1 high-aspect-ratio (HAR) wing [4] are the subject of this study. Importantly, the prototype highly flexible skin is supposed to transfer all the aerodynamic loads to the spar, making the structural behaviour of the latter the one of greatest interest; thus, all experimental tests were performed on the spar alone. The specific aim is to perform the FE model updating of its material parameters (Young's Modulus E, Poisson Ratio ν, density ρ, and damping ratio ζ) in a non-contact way, by extracting the vibrational response of the structure from video acquisitions. These displacement time histories (THs) are compared to the one acquired by a single-point Laser Doppler Vibrometer (LDV), showing good consistency.

The rest of this discussion is organised as follow. In Section 2, the basics of FEM updating are briefly recalled. Section 3 discusses the algorithm applied for the extraction of displacement time histories from the recorded video. In Section 4 the case study of this dynamic investigation is introduced. Section 5 describes the results and Conclusions follow in Section 6

2 FE Model Updating

The concept itself of FE-based Model Updating (FEMU) has been put forward since several decades [5]. A large variety of algorithms have been proposed for this aim at least since the 1990s. A quite exhaustive review can be found in the relatively recent work of Reference [6], while a comparative study is available in Reference [7].

FEMU approaches may be mainly classified as direct and indirect methods; the members of this latter group are also known as sensitivity-based techniques [8]. In direct methods, the individual elements in the system matrices of masses and stiffnesses are adjusted through comparison between the initial model prediction and the experimental data, generally without recurring to iterative algorithms. In the case of indirect techniques, as the name suggests, the adjustments are applied not directly to the system matrices but rather to some specific physical property of the model finite elements. In turn, this causes a variation of the resulting matrices and – hopefully –

brings the predicted output closer to the measured data. The interest audience may refer to the classic book of Friswell & Mottershead [9] for further general information about the topic. A shorter yet effective introduction to indirect techniques can be found in Reference [10].

In the case of this study, an input-output procedure has been applied as an iterative and indirect technique operating in the frequency domain. This approach belongs to the broad family of the response function methods (RFM) [11]. The process is quite straightforward: by taking the recorded inputs and outputs, one or more experimental Frequency Response Functions (FRFs) which define the linear system under exam are compared with the results from the numerical simulations at the same points. This is done here by computing the Normalised Mean Square Error (NMSE) between the numerical and the experimental data in a short frequency range around the first natural frequency. This can be carried out at any output channel of interest, thus allowing a Single-Input Multi-Output (SIMO) characterisation of the investigated system. The iterative algorithm is sketched in the flowchart of Figure 1.

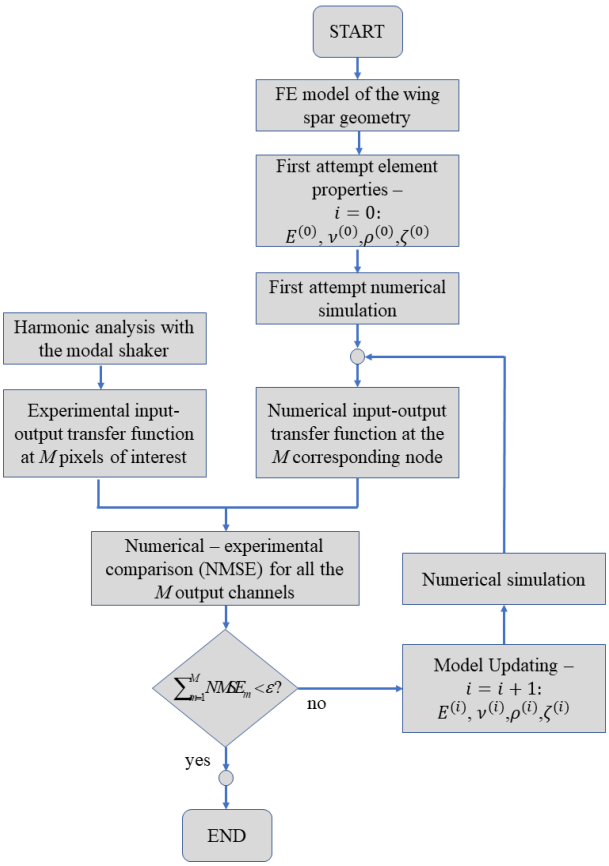

Fig. 1. Flowchart of the iterative FEMU algorithm.

The minimization of the error function was performed on MatLab ® using the `patternsearch()` function, which implements a variant of the generalised pattern search (GPS) algorithm [12]. Convergence was set to occur accordingly to three requirements:

1. cumulative NMSE of all the M output channels considered below an arbitrary limit set to $\varepsilon = 0.01 \cdot M$;
2. change in NMSE less than 0.001 respect to the previous iteration;
3. change in pattern search mesh size less than 10^{-6} respect to the previous iteration.

The FE model of the wing spar (Figure 2), recently used for some related works [13] is made up by 400 8-noded quadratic shell elements, for a total of 1369 nodes, with 6 degrees of freedom per node. The input was applied as a harmonic acceleration to the clamped base, while the output THs were computed at all nodes corresponding to the LDV point of application and close-by investigated cross-sections.

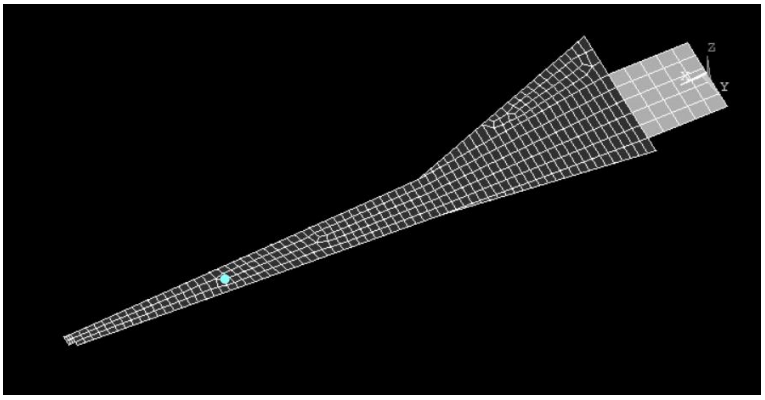

Fig. 2. The geometry of the FE model to be calibrated. The input harmonic excitation was applied to the elements coloured in light grey. The closest node to the LDV dot is highlighted in cyan.

3 Video Acquisition Algorithm

The Virtual Video Vibrometer (VVV) technique, firstly proposed by the Authors in [14], has been utilised here to extract the displacement THs from the video recordings at the cross-sections of interest. The basic concept is that the moving wing edge profile produces a sharp change in the pixel brightness respect to the background, which in turn can be easily detected at any frame. The results are pixel-wise time series of displacements referred to the targeted wing cross-sections, similar to what can be achieved with a Laser Doppler Vibrometer aimed at the same points. As for the LDV, the implicit assumption of this approach is that the trajectory of the transverse motion

can be approximated by a straight line. While this assumption may not hold true for larger transverse deflections [15], this is not an issue when the output amplitude of motion is relatively low, as commonly done for the task of system identification (SI) of structure behaving linearly at low energy levels.

The VVV procedure is very straightforward and can be summarised as follow (all the steps are depicted in Figure 3). Firstly, the original video sequence is converted frame-by-frame to a greyscale image and a frame slice of interest is selected, with arbitrary narrow width, here set at 6 pixels (indicated by the green lines in the top left image of Figure 3). This selection is then isolated (Figure 3, step i) and its brightness is defined at any pixel as 8-bit unsigned integers, thus spanning in a range from a minimum of 0 to a maximum of 256 (step ii). A mean brightness profile is then defined over the six-pixel columns (step iii). The 2-mm-long thickness of the wing spar is noticeable, while the laser dot is revealed by the peak in brightness. Through any nonlinear detrending algorithm, it is then possible to remove the illumination gradient on the background panel (step iv). Here, a Savitzky-Golay sliding polynomial filter [16] of order 3 and window width 27 was applied. This step is also useful to remove any unrelated object included in the frame as long as it is not moving during the recording. At this point, the moving (local or global) maximum can be targeted utilising a peak picking method. The final result is the framewise profile of a Brightness Index (BI). This index is defined as the signed deviation of the brightness respect to the background trend. By following any BI peak of interest frame after frame, the THs of vertical displacement are thus obtained for any given cross-section. While this can be more easily implemented for the most prominent peak, the approach is not limited to it, allowing to select the spar intrados or extrados as well (as long as they are distinguishable from the background at any frame). These THs are finally converted from pixels to millimetres.

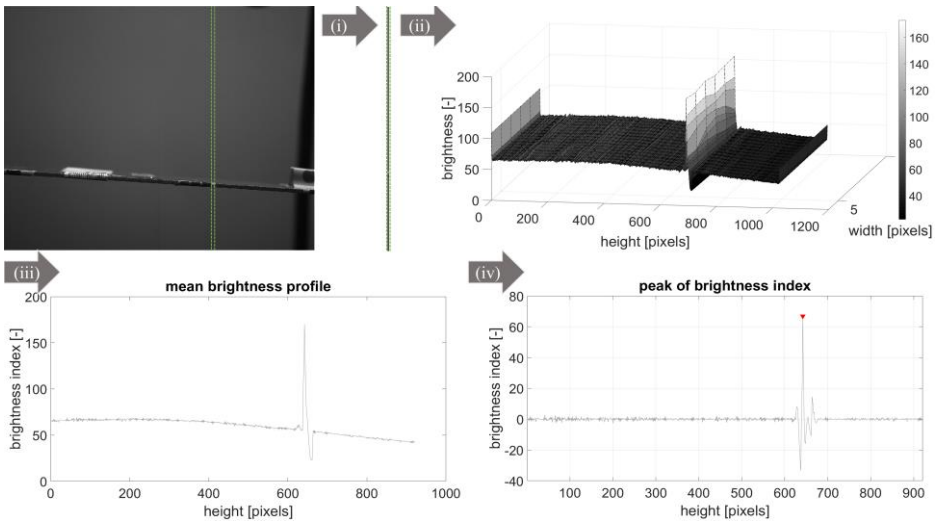

Fig. 3. A pictorial description of the VVV algorithm (steps i – iv).

Respect to the classic LDV acquisitions, this video-based method has both benefits and drawbacks. The main limitation is in terms of spatial resolution, as the accuracy is limited by the pixel dimension and thus depends on the distance of the camera from the target structure (here, the focal length was about 240 mm). This can be improved by several techniques for subpixel resolution and/or by interpolating, for which numerous algorithms exist in the literature. Motion magnification techniques have been proposed in recent years [17], which can be used directly or combined with techniques such as the one described here to obtain displacement THs. Yet, the actual resolution will be inferior respect to the LDV one in most of the cases. On the other hand, the video processing procedure can be applied to any slice of the frame, thus capturing multiple THs from a single experiment. This can be otherwise achieved only employing multi-point LDV, which is much more expensive and difficult to use than single-point LDV or high-speed HD cameras. Moreover, the VVV technique directly measures the displacement of a point, without the need of numerical integration (even if a conversion step from pixel to SI units is still required and can introduce error in the inferred quantities). Another technical issue derives from the internal memory capacity, which is limited and inversely proportional to the pixel density and the frame rate set. In the case of this study, with 1280 x 1024 pixels per frame (width x height), the storage capacity was limited to 4897 frames.

4 Experimental Setup

The whole experimental setup is shown in Figure 4. The studies were performed in the facilities of Cranfield University. The instrumentation is the same as appeared in Reference [18],[19], and [20]; in detail, an Olympus® I-speed 3™ video camera and a Polytec® OFV-505 Sensor Head™ LDV were utilised. More details can be found in Table 2 of Reference [18]. The geometric details of the investigated wing spar are reported in Table 1. The characterisation has been performed via harmonic analysis, by dwelling the spar at its first natural frequency, and with an input acceleration of 0.01 g, low enough to ensure the linearity of the response. The input was applied to the clamped base with a Data Physics® Signal Force™ shaker and directly recorded from its DP760 close-loop™ control software. The camera was set to acquire 2000 frame per second (fps), the same sampling frequency as the laser vibrometer, for better comparability. Thus, the resulting available recording duration is 2.4485 seconds.

The corresponding frequency resolution is therefore limited to 0.4084 Hz, which is relatively coarse yet proved sufficient for the aim of updating the spar FE model. The camera was aimed at the spar trailing edge and the focus was adjusted consequently; the very short focal length can be seen in Figure 4.c. Points on this edge are considered representative of the behaviour of the whole spar at that cross-section (i.e., torsion effects are neglected). This is still viable with negligible effects at very low input amplitudes if the flapwise deflections are the only motion of interest.

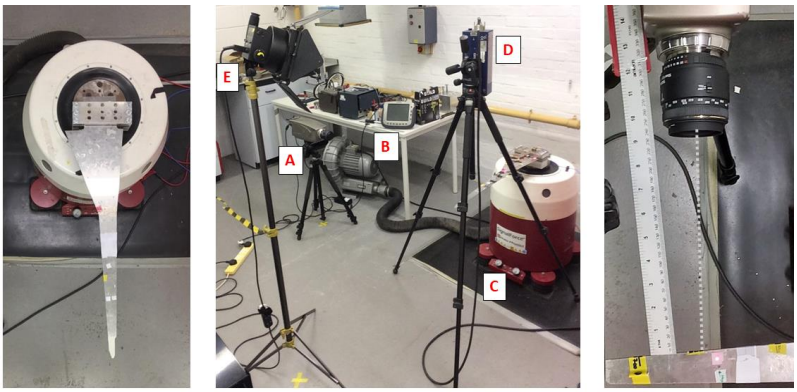

Fig. 4. The experimental setup. (a) top view of the wing spar clamped to the modal shaker. (b) the whole apparatus: the high-speed camera [A] with its acquisition user interface [B], the shaker utilised to apply the input [C], the LDV [D] and the light source [E]. (c) close distance acquisition.

Table 1. Geometrical properties of the wing spar.

Parameter	Value	Measurement unit
Free length (clamp to tip) l_{tip}	706	mm
Thickness t	2	mm
Max width at clamped section $b_{\max}$	180.00	mm
Mid-length width at the section of changing tampering ($l = 258$ mm) $b_{l=258}$	56.10	mm
Min width at the tip section $b_{\min}$	17.04	mm

5 Results

Eleven equally spaced cross-sections, represented in Figure 5 and enlisted in Table 2, were considered. The resulting 11 time series, as well as the derived FRFs of displacement per unit of applied acceleration, are reported in Figure 6 and Figure 7, respectively. Convergence according to the requirements expressed in Section 2 was reached after circa 100 iterations, even if the NMSE Cost Function was already relatively low and almost plateauing after the first 70 iterations. The results are enlisted in Table 3 for the four parameters considered. The values guessed as a first attempt are also reported. For completeness, an early estimation of the parameters, as reported in [18], is included as well. The relatively large divergence in Young's Modulus can be

explained by both the relatively imprecise first estimation and by the non-negligible differences in the experimental setup, especially in the exact position of the clamped cross-section and clamp load. The resulting FRFs are reported in Figure 8. As a validation of the obtained results, it can be seen that the numerically simulated behaviour matches well the experimental results obtained from the LDV acquisition (bottom right corner of Figure 8).

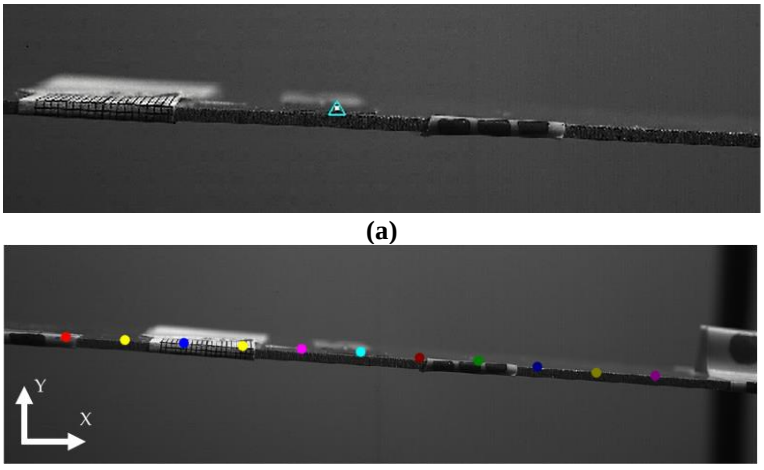

(a)

(b)

Fig. 5. (a) Zoom on the laser dot emanated by the LDV, clearly visible and highlighted in the video recordings. (b) the eleven points investigated along the trailing edge.

Table 2. Location (in pixels) of the selected 6-pixels-wide cross-sections.

Distance from the left border [pixels]	Marker	Distance from the left border [pixels]	Marker	Distance from the left border [pixels]	Marker
106-111		506-511		906-911	
206-211		606-611		1006-1011	
306-311		706-711		1106-1111	
406-411		806-811		LDV: X = 710	

The results of the modal analysis run on the calibrated model are then compared to the experimental findings reported of Pontillo et al [4] in Table 4. It must be remarked that the slight difference is again due to the different experimental setup. In that study, a single vibrometer was applied, thus torsional modes went undetected. The neighbouring 4th flexural flapwise and 1st torsional mode generated some unclear response in their range of frequencies. An unclear result at circa 202 Hz may again be due to imperfectly detected torsion or flection in the chord direction.

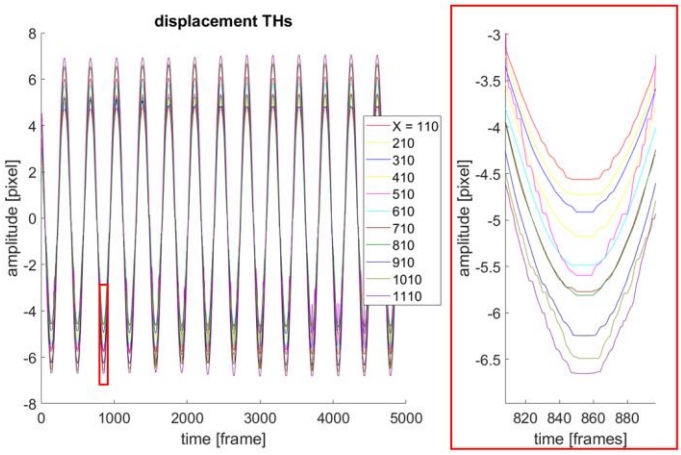

Fig 6. Resulting time histories (pixels amplitude along time expressed in terms of frames). The magnified portion is highlighted in red. The colour scheme reflects the positions highlighted in Figure 5 and Table 2.

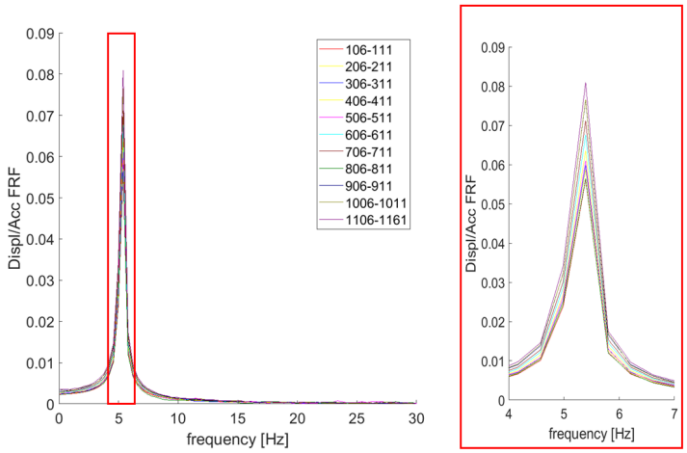

Fig 7. The frequency response function between these displacement outputs and the acceleration input. The colour scheme reflects the positions highlighted in Figure 5 and Table 2.

The experimental investigation of Pontillo et al was upper bounded to 300 Hz, so the 7th flexural flapwise mode most probably fell out of the range. It is noteworthy how the FE Model, while calibrated only on the first mode, can provide a relatively good estimation of all the higher modes for which the comparison with the experimental data is feasible. This proves the reliability of the FE Model, even if it is a very basic and simple approximation of the target plate-like structure. It is important to remark that, as it can be seen from Figure 8, the video-extracted vibrational information is strongly redundant. This is very useful for Model Updating. On one hand, the overdetermination of the problem means that more parameters can be calibrated.

On the other hand, if few parameters have to be estimated, as in this case, extrapolating information from an arbitrarily large amount of closely spaced output channels also makes the resulting system identification more robust than in the case of a single-point LDV.

Table 3. Estimated and Updated mechanical parameters.

Parameter	Early estimates [18]	First attempt assumptions	Final updated values
Young's modulus [MPa]	$73.1000 \cdot 10^3$	$69.1000 \cdot 10^3$	$59.0162 \cdot 10^3$
Density [kg / m^3]	2850.000	2850.000	2893.0649
Damping ratio [%]	-	0.1000	0.8634
Poisson's ratio [-]	0.3300	0.3300	0.2616

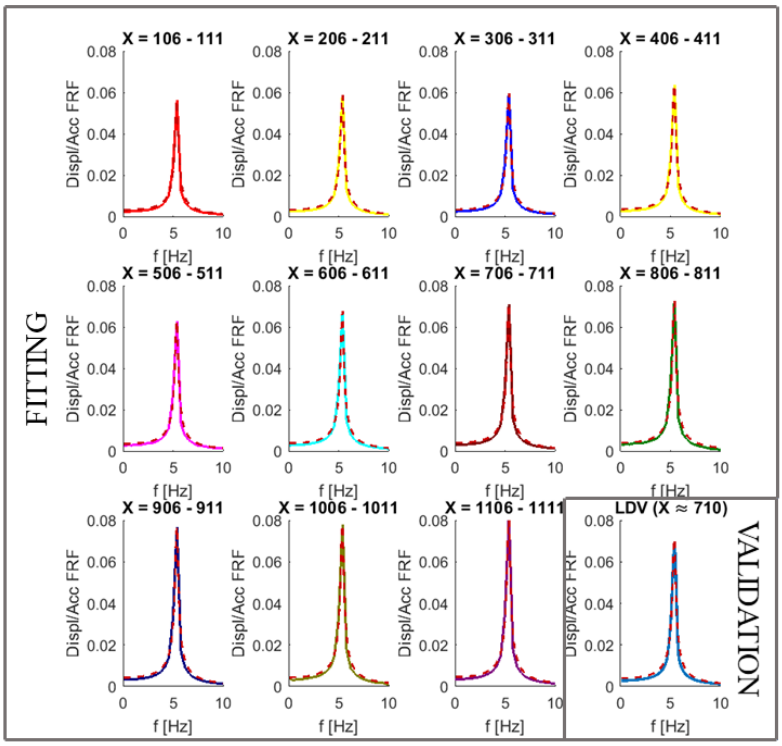

Fig. 8. Results of the fitting procedure at convergence. Numerical FRFs reported as dashed red lines superposed to experimental data from video. Experimental data from the LDV shown for comparison in the bottom right corner.

Table 4. First ten vibrational modes.

ID #	Mode	Experimental values ([4]) [Hz]	Video acquisition [Hz]	Calibrated FE Model [Hz]
1	1st flexural flapwise	5.12	5.40	5.49
2	2nd flexural flapwise	22.02	Out of range	23.16
3	3rd flexural flapwise	55.30	Out of range	55.80
4	4th flexural flapwise	110.10	Out of range	103.99
5	1st torsional	-	Out of range	125.11
6	5th flexural flapwise	174.10	Out of range	172.09
7	1st flexural chord-wise	202.20	Out of range	189.15
8	2nd torsional	-	Out of range	219.90
9	6th flexural flapwise	259.10	Out of range	255.62
10	7th flexural flapwise	Out of range	Out of range	333.89

6 Conclusions

The work presented here detailed a simple yet effective video-based FEMU procedure. The object of this experimental investigation was the spar of a very flexible and HAR wing prototype. This target system was proven in previous studies to be highly affected by the local and global changes in mass due to sensor loading. Therefore, the main difficulty for its dynamical characterisation lies in the invasiveness of the acquisition procedure. Non-contact approaches are very useful from this point of view.

Acknowledgements

The authors would like to thank dr Mudassir Lone for kindly providing the high-speed camera and the wing prototype, and dr Ivan Petrunin and dr Alessandro Pontillo for their help with the experimental setup.

References

1. Civera, M.; Surace, C.; Worden, K. Detection of Cracks in Beams Using Treed Gaussian Processes. In; Springer, Cham, 2017; pp. 85–97.
2. Martucci, D.; Civera, M.; Surace, C.; Worden, K. Novelty Detection in a Cantilever Beam using Extreme Function Theory. *J. Phys. Conf. Ser.* **2018**, *1106*, 012027.
3. Dussart, G.; Portapas, V.; Pontillo, A.; Lone, M. Flight Dynamic Modelling and Simulation of Large Flexible Aircraft. In *Flight Physics - Models, Techniques and Technologies*; InTech, 2018.
4. Pontillo, A.; Hayes, D.; Dussart, G.X.; Lopez Matos, G.E.; Carrizales, M.A.; Yusuf,

S.Y.; Lone, M.M. Flexible High Aspect Ratio Wing: Low Cost Experimental Model and Computational Framework. In Proceedings of the 2018 AIAA Atmospheric Flight Mechanics Conference; American Institute of Aeronautics and Astronautics: Reston, Virginia, 2018.

5. Mottershead, J.E.; Friswell, M.I. Model updating in structural dynamics: A survey. *J. Sound Vib.* **1993**, *167*, 347–375.
6. Sehgal, S.; Kumar, H. Structural Dynamic Model Updating Techniques: A State of the Art Review. *Arch. Comput. Methods Eng.* **2016**, *23*, 515–533.
7. Modak, S. V.; Kundra, T.K.; Nakra, B.C. Comparative study of model updating methods using simulated experimental data. *Comput. Struct.* **2002**, *80*, 437–447.
8. Boscato, G.; Russo, S.; Ceravolo, R.; Fragonara, L.Z. Global Sensitivity-Based Model Updating for Heritage Structures. *Comput. Civ. Infrastruct. Eng.* **2015**, *30*, 620–635.
9. Finite Element Model Updating in Structural Dynamics - Michael Friswell, J.E. Mottershead
10. Mottershead, J.E.; Link, M.; Friswell, M.I. The sensitivity method in finite element model updating: A tutorial. *Mech. Syst. Signal Process.* **2011**, *25*, 2275–2296.
11. Ewins, D.J. Adjustment or updating of models. *Sadhana - Acad. Proc. Eng. Sci.* **2000**, *25*, 235–245.
12. Hooke, R.; Jeeves, T.A. “Direct Search” Solution of Numerical and Statistical Problems. *J. ACM* **1961**, *8*, 212–229.
13. Civera, M.; Ferraris, M.; Ceravolo, R.; Surace, C.; Betti, R. The Teager-Kaiser Energy Cepstral Coefficients as an Effective Structural Health Monitoring Tool. *Appl. Sci.* **2019**, *9*, 5064.
14. Civera, M.; Zanotti Fragonara, L.; Surace, C. Video Processing Techniques for the Contactless Investigation of Large Oscillations. In Proceedings of the proceedings of the AIVELA XXVI Meeting (in publication).
15. Civera, M.; Zanotti Fragonara, L.; Surace, C. Nonlinear Dynamics of Cracked, Cantilevered Beam-like Structures Undergoing Large Deflections. In Proceedings of the metrology for aerospace; 2019.
16. Savitzky, A.; Golay, M.J.E. Smoothing and Differentiation of Data by Simplified Least Squares Procedures. *Anal. Chem.* **1964**, *36*, 1627–1639.
17. Wadhwa, N.; Rubinstein, M.; Durand, F.; Freeman, W.T. Phase-based video motion processing. *ACM Trans. Graph.* **2013**, *32*, 1.
18. Civera, M.; Zanotti Fragonara, L.; Surace, C. Using Video Processing for the Full-Field Identification of Backbone Curves in Case of Large Vibrations. *Sensors* **2019**, *19*, 2345.
19. Civera, M.; Zanotti Fragonara, L.; Surace, C. An experimental study of the feasibility of phase-based video magnification for damage detection and localisation in operational deflection shapes. *Strain* **2020**, e12336.
20. Civera, M.; Calamai, G.; Zanotti Fragonara, L. Experimental Modal Analysis of Structural Systems by Using the Fast Relaxed Vector Fitting Method. Accepted for publication, Structural Control and Health Monitoring 2020.